Materials Physics and Mechanics 43 (2020) 11-17 Received: November 28, 2019

TEMPERATURE EVOLUTION OF THE DIFFUSE REFLECTANCE SPECTRA OF Sr3Bi2O6 STRONTIUM BISMUTHATE

D.S. Shtarev[1]*, E.O. Nashchochin[2], A.V. Syuy[2,3], A.V. Shtareva[1,2]

[1]Yu.A. Kosygin Institute of Tectonics and Geophysics, Far Eastern branch of the Russian Academy of Sciences, 65 Kim Yu Chen Street, Khabarovsk, 680063 Russian Federation

[2]Far Eastern State Transport University, 47 Seryshev Street, Khabarovsk, 680021 Russian Federation

[3]Pacific National University, 136 Tihookeanskaya Street, Khabarovsk, 680035, Russian Federation

*e-mail: shtarev@mail.ru

Abstract. The diffuse reflection spectroscopy (DRS) method was used to study the properties of strontium bismuthate $Sr_3Bi_2O_6$ in a wide temperature range. It is established that after the Kubelka-Munk transformation and logarithmization, it is possible to distinguish three linear sections on the DRS. The presence of such linear regions at energies smaller than the bandgap is usually associated with electron-phonon interactions in the crystal and is described using a model based on the Urbach rule. A high-energy linear region can be associated with a direct transition of electrons from the valence band to the conduction band. The remaining linear sections can be associated with the transfer into the conduction band of electrons biographically localized in deep traps in the bandgap.

Keywords: strontium bismuthate, temperature dependence of diffuse reflection spectra, Urbach rule, Urbach energy, electron-phonon interactions

1. Introduction

The bismuthates of various alkaline earth metals have recently been actively studied as potentially visible light photocatalysts. One of the reasons for this is that they have an anomalous ratio between the potentials of the top of the valence band and the bottom of the conduction band on the one hand, and the bandgap on the other [1]. The most photocatalytic properties of calcium bismuthates [2-10] and strontium bismuthates [11-19] are studied. The most studied barium bismuthate is the composition of BaBiO3 [20-24]. The photocatalytic properties of magnesium bismuthates have yet to be investigated [25].

In the series of bismuthates of the above alkaline earth metals, namely strontium bismuthates are perhaps the most promising photoactive materials. This is due to the fact that they successfully combine high photocatalytic activity and ease of manufacture [11]. On their basis, photocatalysts can be developed for the purification of water and air from organic and inorganic pollutants, for the production of hydrogen due to the photocatalytic decomposition of water, etc. According to theoretical studies [26], the most promising compositions for this are strontium bismuthates, in the cationic sublattice of which the number of strontium atoms exceeds the number of bismuth atoms. That is, such strontium bismuthates, which are located in the phase diagram in the area from 50 to 100 mol.%.

A significant factor limiting the practical use of strontium bismuthates is the relatively large value of the bandgap. Therefore, for strontium bismuthate $Sr_3Bi_2O_6$, the bandgap is 3.2 eV [11]. Such a bandgap makes it impossible to activate the radiation of the visible range. However, it is known that semiconductor photoactive materials can be activated by radiation

http://dx.doi.org/10.18720/MPM.4312020_2

with photon energy less than the bandgap. Such absorption of radiation in an improper region becomes possible due to electron-phonon interactions and is described by the Urbach rule [27]:

$$\alpha = \alpha_0 e^{h\nu/E_U}, \quad (1)$$

where α – semiconductor absorption coefficient, E_U – Urbach energy.

In this work, based on an analysis of the temperature evolution of diffuse reflection spectra, the main parameters of electron-phonon interactions for a promising photoactive material – strontium bismuthate $Sr_3Bi_2O_6$ – are determined.

2. Experimental

Pure strontium bismuthate $Sr_3Bi_2O_6$ was obtained by the solid-phase synthesis in accordance with the procedure described in detail in [11]. Strontium nitrate and bismuth oxide were used as precursors. The precursors were mixed in a stoichiometric ratio, after which they were subjected to two-stage heating: up to 650°C for 24 in the first stage and up to 825°C for 72 hours in the second.

The optical properties of the synthesized strontium bismuthate were studied by diffuse reflection spectroscopy (DRS). Diffuse reflectance spectra were recorded in the temperature range 100–503 K. An Agilent Cary 5000 UV spectrophotometer with an integrating sphere was used to record the DRS. $BaSO_4$ was used as the standard. Also, a special attachment to the spectrophotometer was used, which allows registration of DRS in a vacuum at a controlled temperature. A more detailed description of the design of the device and its capabilities for optical measurements is given in [28].

3. Results and Discussion

Figure 1 shows how the diffuse reflectance spectra of strontium bismuthate $Sr_3Bi_2O_6$ change upon heating from 100 K to 503 K. It can be seen that the largest changes occur in the region of 2.2-3.2 eV.

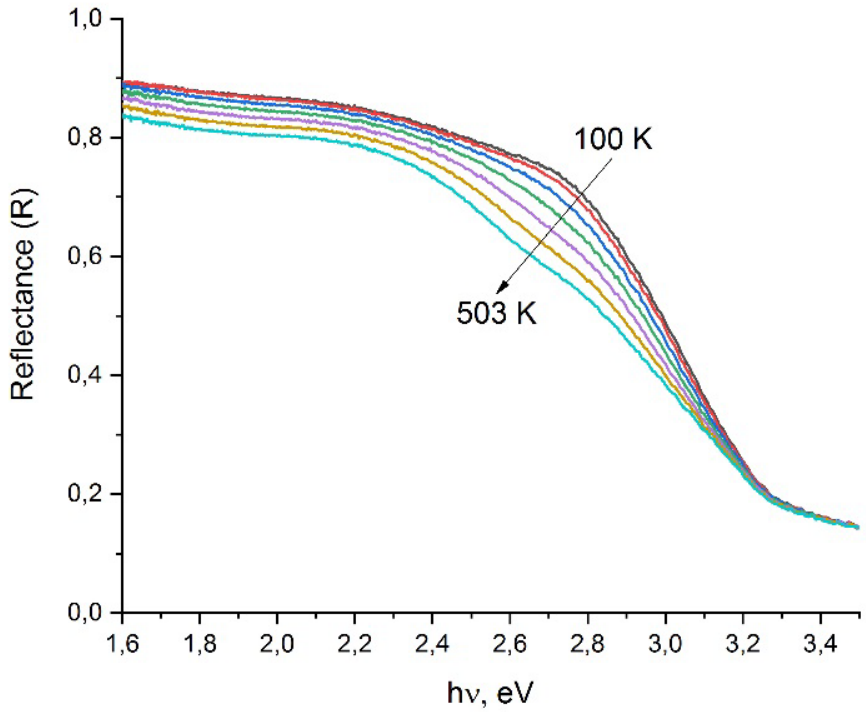

Fig. 1. Temperature evolution of the diffuse reflection spectra of strontium bismuthate $Sr_3Bi_2O_6$ upon heating from 100 K to 503 K

Determining the true absorption coefficient of a semiconductor (see formula 1) is a non-trivial task. Therefore, in practice, to determine the Urbach energy, instead of the absorption coefficient, the Kubelka–Munk function is used [29-30]:

$$F = \frac{(1-R)^2}{2R}. \quad (2)$$

If we logarithm expression (1) and take into account the transition from the absorption coefficient to the Kubelka-Munk function (2), we obtain:

$$\ln(F) = \ln(F_0) + \frac{h\upsilon}{E_U}. \quad (3)$$

Figure 2 presents the diffuse reflectance spectrums, converted by the formula (3). It can be seen that in all the obtained spectra, three linear sections can be distinguished: the first in the region of 2.75-3.3 eV, the second in the region of 2.25-2.75 eV and the third in the region of less than 2.25 eV.

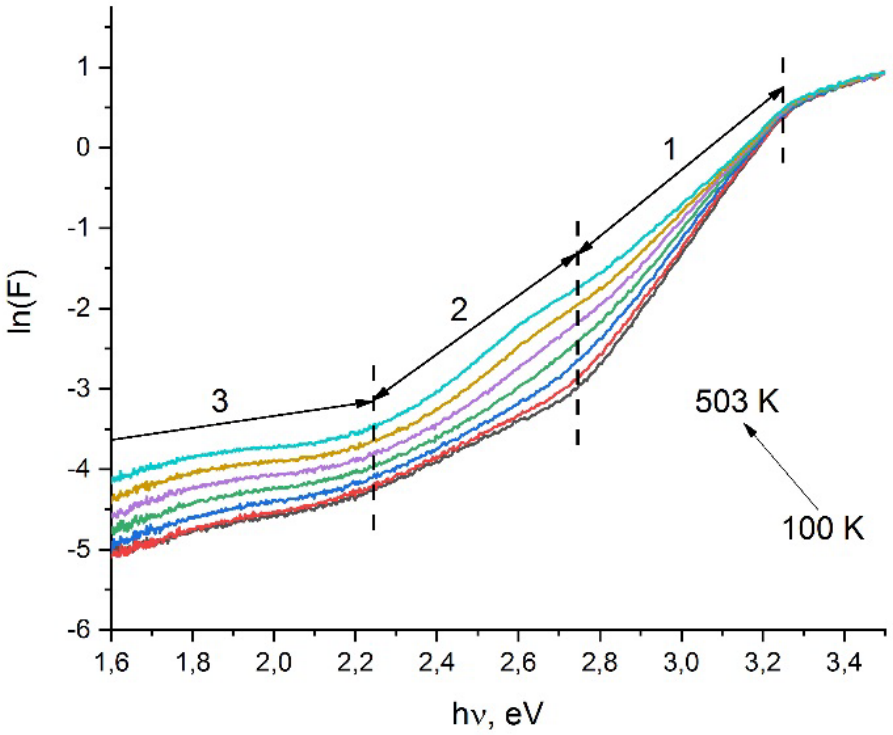

Fig. 2. Kubelka-Munch transformation for diffuse reflectance spectrum of strontium bismuthate $Sr_3Bi_2O_6$ at various temperatures

Each of the detected linear sections is characterized by its own value of the Urbach energy. The energy of Urbach characterizes the ability of an electron to transfer to the conduction band during photoactivation with an energy less than the value of the bandgap. In this case, the photoelectron receives a lack of energy as a result of the electron-phonon interaction from the thermal vibration of the crystal lattice.

The most obvious is the transition of an electron from the valence band to the conduction band. However, from general considerations, transitions into the conduction band of electrons biographically localized in deep traps in the bandgap are also possible. For such electrons, the Urbach rule must also be satisfied. In diffuse reflectance spectrum, such transitions should manifest themselves in the form of additional linear sections in the energy region smaller than the bandgap.

Thus, found and shown in Fig. 2 additional linear sections can be associated with deep defects in the band structure of strontium bismuthate $Sr_3Bi_2O_6$. It follows from expression (3)

that the E_U energy can be found if the linear sections of the curves in Fig. 2 describe by a linear function. The results of such analysis are shown in Fig. 3.

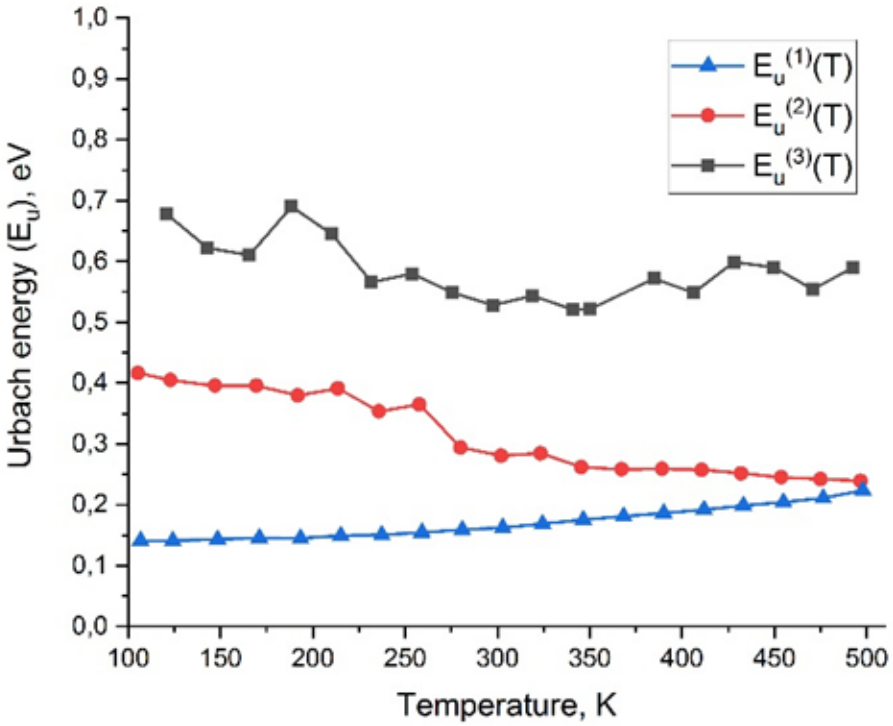

Fig. 3. Temperature dependence of the Urbach energy of strontium bismuthate $Sr_3Bi_2O_6$

The typical temperature dependence of Urbach energy has the following form. At low temperatures, the energy of Urbach is independent of temperature. Usually, this area is attributed to intrinsic or impurity defects. Starting from a certain temperature, a direct relationship is established between Urbach energy and the temperature. This is due to the increase in thermal energy stored by the crystal lattice.

Figure 3 shows that the temperature dependence of the Urbach energy of the first linear section has a well-known and explained, "canonical" form. For the other two linear sections, the temperature dependence of the Urbach energy has a more complex form.

The second linear section is characterized by a constant decrease in the Urbach energy with increasing temperature.

For the third linear section, heating from 100 K to 300 K is accompanied by a decrease in Urbach energy, after which the E_U begins to increase with increasing temperature.

The revealed differences in the temperature dependence of the E_U also confirm that the first linear section of the diffuse reflectance spectrum corresponds to interband transitions, and the second and third are associated with defects in the band structure.

The characteristic of electron-phonon interactions in the crystal lattice can be the steepness parameter (σ), which can be determined by formula (4):

$$\sigma(T) = \frac{kT}{E_U(T)}. \quad (4)$$

Figure 4 shows the calculation results by formula (4) for the temperature dependences of the Urbach energy for the strontium bismuthate $Sr_3Bi_2O_6$ shown in Fig. 3.

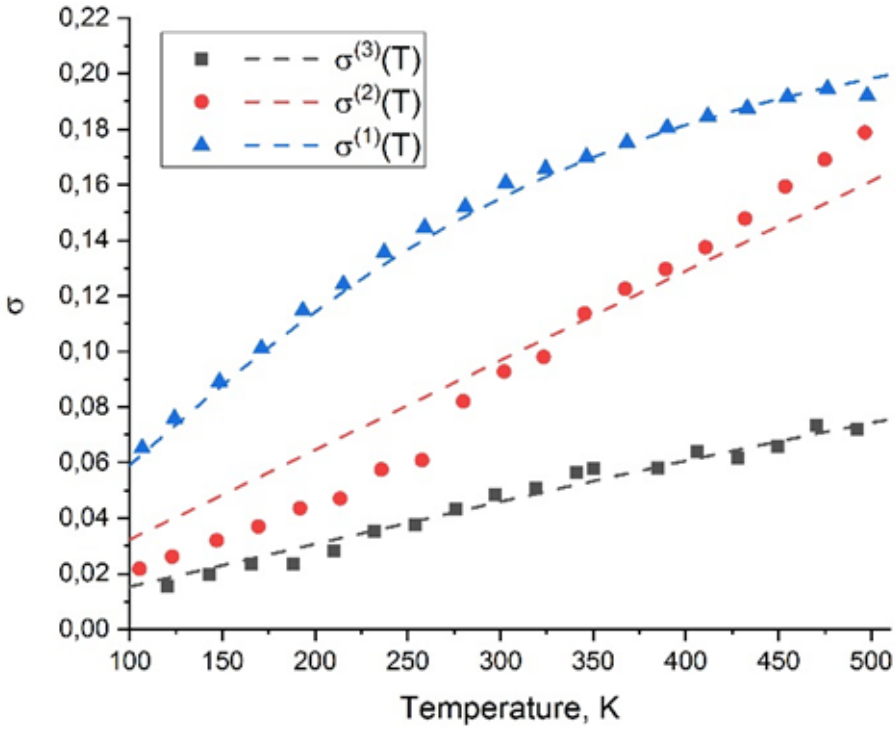

Fig. 4. Temperature dependences of σ for various linear sections of diffuse reflectance spectrum. Markers – experimental data, dashed line – the results of the calculation according to the formula (5), see below

Typical temperature dependence of the steepness parameter σ(T) is described by the following formula [31]:

$$\sigma(T) = \sigma_0 \left(\frac{2kT}{h\nu_p}\right) th\left(\frac{h\nu_p}{2kT}\right), \quad (5)$$

where $h\nu_p$ – is the effective phonon energy, which in most cases coincides with the phonon energy involved in the formation of the long-wave side of the fundamental absorption edge, σ_0 – parameter that describes the optical excitation in the material. In crystalline semiconductors $h\nu_p$ – effective phonon energy in a single-oscillator model that describes an exciton (or electron) – phonon interaction (EPI), and σ_0 – parameter related to the EPI constant g as [32] $\sigma_0 = {}^{2}/_{3g}$.

The obtained experimental data made it possible to determine the main parameters of electron-phonon interactions for all detected linear sections (Table 1).

Table 1. The main parameters of electron-phonon interactions in $Sr_3Bi_2O_6$

Region of Diffuse Reflectance Spectrums	$h\nu_p$, meV	σ_0	g
I linear section (2.75-3.3 eV)	70	0.24	2.7(7)
II linear section (2.25-2.75 eV)	930	1.74	0.38
III linear section (<2.25 eV)	180	0.16	4.1(6)

4. Conclusion

The studies performed allowed us to establish linear sections in the Diffuse Reflectance Spectrums that are associated with both interband transitions and deep biographical defects in the band structure of strontium bismuthate $Sr_3Bi_2O_6$. Applying the Urbach rule to the detected linear sections made it possible to determine the main parameters of electron-phonon interactions.

Acknowledgments. *The research was carried out at the expense of a grant from the Russian Science Foundation (project No. 19-73-10013).*

References

[1] Shtarev DS, Shtareva AV, Ryabchuk VK, Rudakova AV, Serpone N. Considerations of Trends in Heterogeneous Photocatalysis. Correlations between conduction and valence band energies with bandgap energies of various photocatalysts. *ChemCatChem*. 2019;11(15): 3534-3541.

[2] Shtarev DS, Ryabchuk VK, Makarevich KS, Shtareva AV, Blokh AI, Astapov IA, Serpone N. Calcium Bismuthate Nanoparticulates with Orthorhombic and Rhombohedral Crystalline Lattices: Effects of Composition and Structure on Photoactivity. *ChemistrySelect*. 2017;2(30): 9851-9863.

[3] Montalvo-Herrera T, Sanchez-Martinez D, Torres-Martinez LM. Sonochemical synthesis of $CaBi_6O_{10}$ nanoplates: photocatalytic degradation of organic pollutants (ciprofloxacin and methylene blue) and oxidizing species study (h^+, •OH, H_2O_2 and O_2^{-}•). *Journal of Chemical Technology & Biotechnology*. 2017;92(7): 1496-1502.

[4] Liu Z, Wang X, Cai Q, Ma C, Tong Z. $CaBi_6O_{10}$: a novel promising photoanode for photoelectrochemical water oxidation. *Journal of Materials Chemistry A*. 2017;5(18): 8545-8554.

[5] Shtarev DS, Shtareva AV, Syuy AV, Pereginyak MV. Synthesis and photocatalytic properties of alkaline earth metals bismuthates – bismuth oxide compositions. *Optik - International Journal for Light and Electron Optics*. 2016;127(3): 1414-1420.

[6] Shtarev DS, Doronin IS, Blokh AI, Shtareva AV. Dependency of the optical properties of heterogeneous calcium bismuthate – bismuth oxide particles on the order of layers alternation. *Optical and Quantum Electronics*. 2016;48(7): 365.

[7] Shtarev DS, Shtareva AV. Dependence of optical properties of calcium bismuthates on synthesis conditions. *Journal of Physics: Conference Series*. 2016;735(1): 012068.

[8] Wang Y, He Y, Li T, Cai J, Luo M, Zhao L. Photocatalytic degradation of methylene blue on $CaBi_6O_{10}/Bi_2O_3$ composites under visible light. *Chemical Engineering Journal*. 2012;189-190: 473-481.

[9] Wang Y, He Y, Li T, Cai J, Luo M, Zhao L. Novel $CaBi_6O_{10}$ photocatalyst for methylene blue degradation under visible light irradiation, Catalysis Communications. 2012;18: 161-164.

[10] Tang JW, Zou ZG, Ye JH. Efficient photocatalytic decomposition of organic contaminants over $CaBi_2O_4$ under visible-light irradiation. *Angew.Chem.Int.Ed*. 2004;43(34): 4463-4466.

[11] Shtarev DS, Shtareva AV, Ryabchuk VK, Rudakova AV, Murzin PD, Molokeev MS, Koroleva AV, Blokh AI, Serpone N. Solid-State Synthesis, Characterization, UV-Induced Coloration and Photocatalytic Activity – The $Sr_6Bi_2O_{11}$, $Sr_3Bi_2O_6$ and $Sr_2Bi_2O_5$ Bismuthates. *Catalysis Today*. 2020;340: 70-85.

[12] Shtarev DS, Shtareva AV, Molokeev MS, Syuy AV, Nashchochin EO. About Photocatalytic Properties of some Heterostructures Based on Strontium Bismuthate. *Key Engineering Materials*. 2019;806: 161-166.

[13] Shtarev DS, Shtareva AV, Mikhailovski VJ, Nashchochin EO. On the influence of strontium carbonate on improving the photo-catalytic activity of strontium bismuthate $Sr_6Bi_2O_{11}$. *Catalysis Today*. 2019;335: 492-501.

[14] Obukuro Y, Matsushima S, Obata K, Suzuki T, Arai M, Asato E, Okuyama Y, Matsunaga N, Sakai G. Effects of La doping on structural, optical, electronic properties of $Sr_2Bi_2O_5$ photocatalyst. *Journal of Alloys and Compounds*. 2016;658: 139-146.

[15] Yang YC, Wang X, Qu J. Preparation and photocatalytic degradation of malachite green by photocatalyst $SrBi_4O_7$ under visible light irradiation. *Applied Mechanics and Materials*. 2014;522-524: 411-415.
[16] Zhou W, Yu X. Use of $Sr_2Bi_2O_5$ as photocatalyst for the degradation of acid red G. *Desalination and Water Treatment*. 2011;30(1-3): 295-299.
[17] Shan Z, Xia Y, Yang Y, Ding H, Huang F. Preparation and photocatalytic activity of novel efficient photocatalyst $Sr_2Bi_2O_5$. *Materials Letters*. 2009;63(1): 75-77.
[18] Hu X, Hu C, Qu J. Photocatalytic decomposition of acetaldehyde and Escherichia coli using $NiO/SrBi_2O_4$ under visible light irradiation. *Applied Catalysis B: Environmental*. 2006;69(1-2): 17-23.
[19] Hu C, Hu X, Guo J, Qu J. Efficient destruction of pathogenic bacteria with $NiO/SrBi_2O_4$ under visible light irradiation. *Environmental Science & Technology*. 2006;40(17): 5508-5513.
[20] Ge J, Yin WJ, Yan Y. Solution-Processed Nb-Substituted $BaBiO_3$ Double Perovskite Thin Films for Photoelectrochemical Water Reduction. *Chemistry of Materials*. 2018;30(3): 1017-1031.
[21] Weng B, Xiao Z, Meng W, Grice CR, Poudel T, Deng X, Yan Y. Bandgap Engineering of Barium Bismuth Niobate Double Perovskite for Photoelectrochemical Water Oxidation. *Advanced Energy Materials*. 2017;7(9): 1602260.
[22] Khraisheh M, Khazndar A, Al-Ghouti MA. Visible light-driven metal-oxide photocatalytic CO_2 conversion. *International journal of energy research*. 2015;39(8): 1142-1152.
[23] Yan B, Jansen M, Felser C. A large-energy-gap oxide topological insulator based on the superconductor $BaBiO_3$. *Nature Physics*. 2013;9: 709-711.
[24] Tang J, Zou Z, Ye J. Efficient Photocatalysis on $BaBiO_3$ Driven by Visible Light. *The Journal of Physical Chemistry C*. 2007;111(34): 13779-13785.
[25] Ropp RC. *Encyclopedia of the alkaline earth compounds*. Elsevier; 2013.
[26] Shtarev DS, Blokh AI, Nashchochin EO, Shtareva AV. The dependence of the conduction band edge of the alkali earth metal bismuthates on their composition. *Optical and Quantum Electronics*. 2018;50: 228.
[27] Urbach F. The Long-Wavelength Edge of Photographic Sensitivity and of the Electronic Absorption of Solids. *Physical Review*. 1953;95(5): 1324-1333.
[28] Kuznetsov VN, Glazkova NI, Mikhaylov RV, Serpone N. In situ study of photo- and thermo-induced color centers in photochromic rutile TiO_2 in the temperature range 90-720 K. *Photochemical and Photobiological Sciences*. 2016;15(10): 1289-1298.
[29] Kubelka P, Munk F. Ein Beitrag zur Optik der Farbanstriche. *Zeitschrift für Technische Physik*. 1931;12: 593-601.
[30] Kubelka P. New contributions to the optics intensely light-scattering materials. Part I. *Journal of the Optical Society of America*. 1948;38(5): 448-457.
[31] Studenyak I, Kranjcec M, Kurik M. Urbach Rule in Solid State Physics. *International Journal of Optics and Applications*. 2014;4(3): 76-83.
[32] Kurik MV. Urbach rule (Review). *Physica Status Solidi (A)*. 1971;8(1): 9-45.